



Improvement of the Global Connectivity using Integrated Satellite-Airborne-Terrestrial Networks with Resource Optimization

Item Type	Article
Authors	Alsharoa, Ahmad;Alouini, Mohamed-Slim
Citation	Alsharoa, A., & Alouini, M.-S. (2020). Improvement of the Global Connectivity using Integrated Satellite-Airborne-Terrestrial Networks with Resource Optimization. IEEE Transactions on Wireless Communications, 1-1. doi:10.1109/twc.2020.2988917
Eprint version	Post-print
DOI	10.1109/TWC.2020.2988917
Publisher	Institute of Electrical and Electronics Engineers (IEEE)
Journal	IEEE Transactions on Wireless Communications
Rights	(c) 2020 IEEE. Personal use of this material is permitted. Permission from IEEE must be obtained for all other users, including reprinting/ republishing this material for advertising or promotional purposes, creating new collective works for resale or redistribution to servers or lists, or reuse of any copyrighted components of this work in other works.
Download date	2024-04-17 06:48:29
Link to Item	http://hdl.handle.net/10754/660721

Improvement of the Global Connectivity using Integrated Satellite-Airborne-Terrestrial Networks with Resource Optimization

Ahmad Alsharoa, *Senior Member, IEEE*, and Mohamed-Slim Alouini, *Fellow, IEEE*

Abstract

In this paper, we propose a novel wireless scheme that integrates satellite, airborne, and terrestrial networks aiming to support ground users. More specifically, we study the enhancement of the achievable users' throughput assisted with terrestrial base stations, high altitude platforms (HAPs), and satellite station. The goal is to optimize the resource allocations and the HAPs' locations in order to maximize the users' throughput. In this context, we propose to solve the optimization problem in two stages; first a short-term stage and then a long-term stage. In the short-term stage, we start by proposing a near optimal solution and low complexity solution to solve the associations and power allocations. In the first solution, we formulate and solve a binary linear optimization problem to find the best associations and then using Taylor expansion approximation to optimally determine the power allocations. While in the second solution, we propose a low complexity approach based on frequency partitioning technique to solve the associations and power allocations. On the other hand, in the long-term stage, we optimize the locations of the HAPs by proposing an efficient algorithm based on a recursive shrink-and-realign process. Finally, selected numerical results show the advantages provided by our proposed optimization scheme.

Index Terms

Terrestrial base stations, high altitude platforms, satellite station, optimization.

Ahmad Alsharoa is with the Electrical and Computer Engineering Department, Missouri University of Science and Technology, Rolla, Missouri 65409, USA, E-mail: aalsharoa@mst.edu.

Mohamed-Slim Alouini is with the Computer, Electrical and Mathematical Sciences and Engineering (CEMSE) Division, King Abdullah University of Science and Technology (KAUST), Thuwal, Makkah Province, Saudi Arabia. E-mails: slim.alouini@kaust.edu.sa.

I. INTRODUCTION

A. Background

With the rapid growth in mobile and wireless devices in addition to huge data traffic, the traditional terrestrial network is expected to face difficulties in supporting the demands of the users. In addition, it is infeasible to develop terrestrial infrastructure in remote areas to provide telecommunication services. To mitigate these limitations, integrating the current terrestrial network with high altitude stations has become necessary to provide global connectivity.

Integrating the terrestrial network with the space network, including satellite stations, is one of the proposed solutions in order to increase the network's coverage and capacity. Several techniques have been studied in the literature including using multiple spot beams at the satellite station associated with multiple protocol label switching and spectrum access controlled [1], [2]. For instance, In [1], a cooperative scheme based on non-orthogonal multiple access has been proposed, where the satellite station communicates with the users via the help of terrestrial base station (TBS) working as a relay. While in [2], the authors propose to use TBSs as amplify relays to maintain the communication links between multiple satellite stations and multiple users. Furthermore, several spectrum resources techniques have been investigated recently to improve the communication link by utilizing the spectrum in efficient ways such as allocating the system resources to hot beams in order to meet user demands or to address adverse channels [3]–[5]. For example, in [5], the spectrum management scheme of satellite-terrestrial integration is proposed to address the unpredictable demands of users associated with the satellite station. The authors in this work introduced a hunger marketing strategy that manages the spectrum to influence users behavior in bandwidth planning and benefit satellite system meanwhile. Therefore, allowing a more efficient dynamic spectrum management.

However, all traditional satellite communications techniques are constrained due to the high path-loss attenuation of the communication links between the satellite stations and the ground users. In addition to that, the satellite stations can be located in various orbital heights and, thus, causing extra delay when providing real-time services to ground users. To fill the gap, High altitude platforms (HAPs) such as airships and balloons operating in the stratosphere, at altitude of 17 Km to 20 Km, can be a promising wireless solution that is expected to work along with the existed satellite and terrestrial networks [6]. This altitude range is chosen because of its low wind currents and low turbulence which reduces the energy consumptions aiming to

maintain the position of the HAP. Therefore, HAPs can act as aerial base stations to improve the communication links between satellite stations and ground users and hence improve the overall network throughput. This satellite-airborne-terrestrial integrated system can be part of civilian life with high-reward opportunities in improving the wireless utilization and provisioning better wireless access for public safety and first responders.

B. Related Works

HAPs acting as wireless BSs have been proposed to help the global connectivity [7], [8]. The main advantages of using HAPs over the TBSs can be summarized as follows [6], [9]:

- High coverage area: The broadband coverage area of TBSs (coverage area radius around 1000 m) is usually limited compare to HAPs (coverage area radius around 30 Km) due to large non-line-of-sight pathloss. Thus, only few HAPs can cover some small countries [10].
- Dynamic and quick deployment: The HAPs have the ability to fly to infrastructure-less regions in order to enable on-demand services.
- Low energy consumptions: The HAPs can be equipped with solar panels that collecting energy during the daytime. Thus, with a careful trajectory optimization, HAPs can be self powered [11], [12].

On the other hand, the main advantages using HAPs over the satellite stations can be summarized as follows [7]

- Quick and low cost deployment: HAPs can accommodate temporal and traffic demand quickly, where one HAP is enough to start the service. Also, HAPs can play a significant role in emergency or disaster relief applications by flying to desired areas, in short timely manner, in order to restart the communications [13]. In addition, the deployment cost of the HAPs is much less than the satellite deployment cost.
- Low propagation delays and strong signals: Due to the high path-loss attenuation between satellite stations and ground users, HAPs can provide services to ground users in lower delay [8].

Several papers in the literature have studied the deployment of the HAPs [11], [12], [14]. For instance, the work proposed in [14] investigates the HAPs' deployment taking into consideration the quality-of-service (QoS) of ground users. The authors propose a self-organized game theory model, where the HAPs are modeled as rational and self-organized players with the goal of

achieving optimal configuration of the HAPs that maximizing the users' QoS. While the work in [11], propose trajectory optimization techniques for HAPs equipped with solar power panels. More specifically, the authors in [11], proposed a greedy heuristic and realtime solution to optimize the HAPs' trajectory by minimizing the consumed energy which is constrained by the amount of the harvested energy. In [12], the authors extended their work presented in [11], to include several trajectory optimization methods aiming to maximize the storage energy in HAPs instead of minimizing the consumed energy.

Furthermore, improving the system throughput has been considered as another important key factors in HAPs communications. The authors in [15], propose multicast system model that uses orthogonal frequency division multiple access (OFDMA) to find the best transmit powers, time slots, and sub-channels in order to maximize the total ground users' throughput. In other words, the goal was to maximize the number of users that receive the requested multicast streams in the HAP service area in a given OFDMA frame. The improvement of the multiple HAPs' capacity is presented in [16], where the authors show that the HAPs can offer a spectrally efficiency by exploiting the directionality of the user antenna. In other words, the authors explained how multiple HAPs can share the same frequency band by taking the advantage of the users' antenna directionality. In [17], the authors investigated the multi-user multiple-input multiple-output (MU-MIMO) in HAP communication, where the HAPs are equipped with large-scale antenna arrays. The goal was to formulate and solve a low computational complexity technique that maximizes the signal-to-interference-noise ratio (SINR) and limits the interference between users. However, all these works have not considered the back-hauling (BH) link for the HAPs.

Few research in the literature have considered the integration between satellite, airborne, and terrestrial networks [18], [19]. For instance, the work in [18], consider using HAP as a relay to enhance the satellite link. The goal was to reduce the total energy consumption while achieving certain downlink users' QoS from the satellite. While the authors in [19], present the idea of bidirectional function offloading and its possible applications by exploring the full advantages of integrated networks. More specifically, the work studied the virtual network functionality and service function chaining that enabling network reconfiguration framework.

C. Contributions

This paper studies the resource allocation with front-hauling (FH) and back-hauling (BH) associations in order to improve the global connectivity using satellite, airborne, and terrestrial

networks integration. Satellite station and HAPs can play significant role in global connectivity in the case when the TBSs are overloaded or to support users with high throughput located outside the TBSs coverage areas (e.g., suburban and remote areas). The objective of the proposed framework is to improve the downlink throughput of the ground users while respecting the resource limitations. To the best of our knowledge, the problem of resource, power management, and associations (including FH and BH associations) for satellite, airborne, and terrestrial networks integration has not been discussed so far. The main contributions of this work can be summarized as follows:

- The objective is to support the terrestrial network with satellite station and HAPs in order to enhance the network performance. In our framework, an optimization problem is formulated aiming to maximize the downlink users' throughput while taking into account the power budgets limitation, associations, and BH constraints.
- We formulate two problems based on how often optimizing the parameters: short-term stage and long-term stage. In the short-term stage, we solve the FH and BH associations and power allocations with fixed HAPs' location. In long-term stage, and based on average users distribution, we optimize the locations of the HAPs. In other words, the short-term stage variables can be optimized frequently, while the long term stage variables can be optimized in long time periods.
 - Short-term stage: Due to the non-convexity of the formulated problem, we propose two solutions. In the first solution, we start by jointly optimize the FH and BH association given fixed transmit power levels. Then, optimizing the transmit powers using Taylor expansion approximations. In the second solution, we propose a low complexity solution based on frequency partitioning (FP) technique to optimize the associations and transmit powers.
 - Long-term stage: We propose an efficient and low complexity heuristic algorithm based on shrink-and-realign (SR) process to optimize the locations of the HAPs. Note that, this algorithm will be optimized once every long time frame.
- We consider different users objective functions utilities depending on the level of fairness among users.
- Finally, we analyze the performance of our proposed scheme under different system parameters.

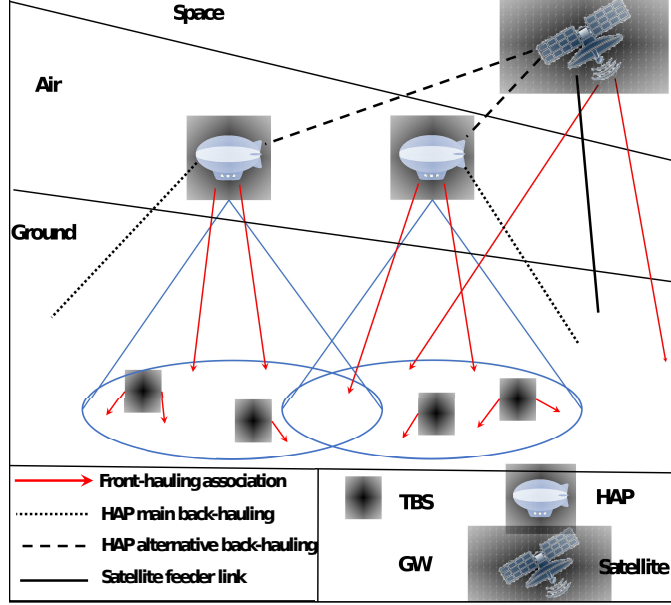


Fig. 1: System model.

D. Paper Organization

The remainder of this paper is organized as follows. Section II provides the system model. The problem formulation is given in Section III. Section IV describes the short-term stage by optimizing the associations and power allocation solutions. Section V gives the long-term stage by optimizing the locations of the HAPs. The numerical results are discussed in Section VI. Finally, the paper is concluded in Section VII.

II. SYSTEM MODEL

We consider an integrated communication network consisting of three tiers: (i) space tier with one satellite station, (ii) air tier with L HAPs, and (iii) ground tier with M TBS. In addition, we also consider W gate ways (GWs) feeder stations to be used for the BH. We aim to provide downlink communications to U ground users in a certain geographical area as shown in Fig. II. In Table I, we summarize the main notations used in this paper.

A. Assumptions

We assume that the OFDMA technique is adopted. The available spectrum is divided into number of resource blocks (RBs), where each RB in tier S has a bandwidth of B^S Hz [20]. We assume that there is no interference between different tiers, where the available bandwidth

TABLE I: List of Notations

Notation	Description
U	Number of users
M	Number of TBSs
L	Number of HAPs
W	Number of GWs
N^S	Number of available RBs at tier S
\mathbf{J}_u^U	User geographical coordinates
\mathbf{J}_s^S	BS s geographical coordinates in tier S
$h_{su,n}^S$	FH channel gain between BS s and user u over RB n
g_{xy}	BH channel gain between x and y
A_{su}^S	Attenuation gain due to environment effect
$\Omega_0, \Omega_1, \Omega_2$	Shadowed Rician fading parameters
κ_L	Rician fading parameter
$\epsilon_{su,n}^S$	A binary variable indicates the FH association between BS s and user u over RB n
δ_{wl}	A binary variable indicates the BH association between GW w and HAP l
$P_{su,n}^S$	FH transmit power of BS s over RB n
P_0	BH transmit power
B^S	FH bandwidth of BS s in tier S
B_0	BH bandwidth
\mathcal{N}_0	Noise power
$R_{su,n}^S$	FH data rate from BS s to user u over RB n
\bar{R}_{wl}	BH data rate from GW w to HAP l
T	Maximum shrink-and-realign iterations

is divided sparsely between these tiers. We denote by N^S the number of available RBs at tier S (i.e., $S = 0$ for the space tier and $S = L$ for the air tier, and $S = M$ for the ground tier). In addition to the above assumption, we make the following practical assumptions: (i) a user is served at most by one BS¹ using only one RB. (ii) there is no intra-cell interference on the downlink between users associated to the same BS as they are using different sets of orthogonal RBs. (iii) an inter-cell interference between users associate to different TBSs in the ground tier (i.e., a TBS with nearby TBSs). On the other hand, we ignore this interference in the space

¹We refer to BS as TBS, HAP, or satellite station.

and air tiers because the satellite station and HAPs can be equipped with different antennas and different beams where they allow managing the resources in an efficient way by using different frequency sets (FSs) [16]. Note that the antennas of HAPs are arranged to produce a regular hexagonal structure, where multiple beam antenna payload at each HAP serve multiple ground cells as shown in Fig. 2.

B. Channel Model

We consider a 3D coordinate system where the coordinate of user u , BS s are given, respectively, as $\mathbf{J}_u^U = [x_u^U, y_u^U, 0]'$, $\mathbf{J}_s^S = [x_s^S, y_s^S, z_s^S]'$, $S \in \{M : \text{for TBSs}, L : \text{for HAPs}, 0 : \text{for satellite station}\}$, where $[\cdot]'$ denotes the transpose operator.

1) *Front-hauling Channel Model:* Taking into account the fading and shadowing fluctuations in addition to the pathloss, the channel gain between BS s and user u can be modeled as:

$$h_{su,n}^S = \left(\frac{C}{4\pi d_{su}^S f_c^S} \right)^2 A_{su}^S F_{su,n}^S, \quad (1)$$

where C and f_c^S are the speed of light and carrier frequency in tier S , respectively. d_{su}^S is the distance between BS s in tier S and user u . In (1), the first factor $(C/4\pi d_{su}^S f_c^S)^2$ captures propagation and path-loss and the second A_{su}^S is the attenuation gain due to environment effects which depends on the distance between the BS s and user u and given as [15], [21]:

$$A_{su}^S = \begin{cases} A_{mu}^M = 1 & , \text{ for ground tier,} \\ A_{lu}^L = 10^{\frac{3d_{lu}^L \chi}{10z_l^L}} & , \text{ for air tier,} \\ A_{0u}^0 = 10^{\frac{3d_{0u}^0 \chi}{10z_0^0}} & , \text{ for space tier,} \end{cases} \quad (2)$$

where χ is the attenuation factor due to environment effects such as rain, wind, cloud, etc. The last factor in (1), $F_{su,n}^S$, corresponds to fading distribution between BS s in tier S and user u over RB n . For the ground tier (i.e., $S = M$, $s = m$), $F_{su,n}^S$ corresponds to Rayleigh fading power between TBS m and user u with a Rayleigh parameter a such that $E\{|a|^2\} = 1$. For the air tier (i.e., $S = L$, $s = l$), $F_{su,n}^S$ is the Rician small scale gain between HAP l and user u over RB n with Rician factor equal to κ_L [15], [22]. Finally, for the space tier (i.e., $S = 0$, $s = 0$), the $F_{su,n}^S$ is assumed as shadowed Rician fading based on $(\Omega_0, \Omega_1, \Omega_2)$, where Ω_0 , and $2\Omega_1$ are the average power of the line-of-sight (LoS) component and of the multipath component, respectively. Ω_2 is a Nakagami parameter ranging from 0 to ∞ that shows the intensity of the fading [23]. Without loss in generality, fast fading is assumed to be approximately constant over the subcarriers of a given RB, and independent identically distributed (i.i.d) over RBs.

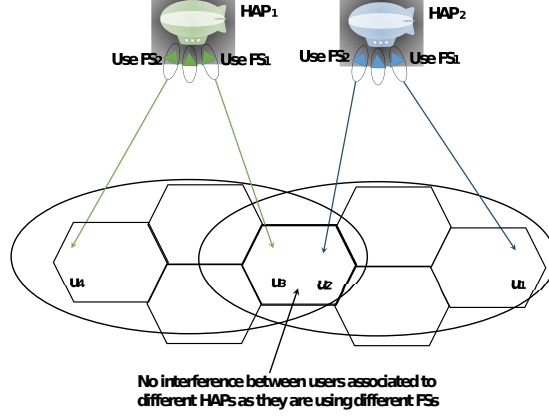


Fig. 2: Location of the HAPs.

2) *Back-hauling Channel Model*: We assume that the BH channel gain between x and y stations, i.e., between GW ($x = w$) HAP l ($y = l$) for the main BH link, and between satellite station ($x = 0$) and HAP l ($y = l$) for the alternative BH link, can be given as [15], [22], [24], [25]

$$g_{xy} = \left(\frac{C}{4\pi d_{xy} f_c} \right)^2 A_{xy} F_{xy}, \quad (3)$$

where F_{xy} , corresponds to Rician fading distribution between x and user y with Rician factor equal to κ_{xy} . The choice of κ_{xy} will be depends on the main or alternative BH links.

C. Front-hauling Association

A ground user can be associated with only one BS (i.e., either a TBS, HAP, or satellite station) at a certain time. Therefore, we introduce a binary variable $\epsilon_{su,n}^S$, where $S \in \{M, L, 0\}$, $s \in \{m, l, 0\}$ for TBS m , HAP l , and satellite station, respectively, is equal to 1 if BS s is associated with user u over the RB n and 0 otherwise, and is given as follows:

$$\epsilon_{su,n}^S = \begin{cases} 1, & \text{if BS } s \text{ is associated with user } u \text{ over RB } n. \\ 0, & \text{otherwise.} \end{cases} \quad (4)$$

We assume that each BS can be associated with multiple users. On the other hand, each user can be associated with one BS at most using one RB. Hence, the following condition should be respected:

$$\sum_{S \in \{M, L, 0\}} \sum_{s=1}^S \sum_{n=1}^{N^S} \epsilon_{su,n}^S \leq 1, \quad \forall u. \quad (5)$$

In addition, in order to mitigate the intra-cell interference inside each cell corresponding to BS s in tier S , we assume that different RBs are allocated to different users that associated with same BS s . Therefore, the following condition should be satisfied, respectively:

$$\sum_{u=1}^U \epsilon_{su,n}^S \leq 1, \quad \forall s, \forall S, \forall n = 1, \dots, N^S. \quad (6)$$

D. Back-hauling Association

It is assumed that HAP l can be associated with either GW w as a main BH link or with the satellite station as an alternative BH link based on the users distributions and the quality of the BH link as shown in Fig. II. Therefore, we introduce another binary variable δ_{wl} for the BH association where δ_{wl} ($w = 0$ for satellite station and $w = 1, \dots, W$ for GWs) is equal to 1 if HAP l is associated with station w and 0 otherwise. Without loss of generality, we assume that each HAP should be strictly associated with one station (either one GW or satellite station). Therefore, the following equality should be respected:

$$\sum_{w=0}^W \delta_{wl} = 1, \quad \forall l. \quad (7)$$

Finally, we denote by \bar{L}_w the maximum number of HAPs that can be associated to station w in the BH, such that:

$$\sum_{l=1}^L \delta_{wl} \leq \bar{L}_w \quad \forall w. \quad (8)$$

E. Downlink Data Rates

It is assumed that the total spectrum is shared sparsely between tiers. The achievable FH data rate of user u served from a BS S , where $S \in \{M, L, 0\}$, over RB n can be given as:

$$R_{su,n}^S = B^S \epsilon_{su,n}^S \log_2 \left(1 + \frac{P_{su,n}^S h_{su,n}^S}{\mathcal{I}_{su}^S + \mathcal{N}_0 B^S} \right), \quad (9)$$

where $P_{su,n}^S$ is the BS transmitted power allocated to RB n , \mathcal{N}_0 is the noise power, and \mathcal{I}_{su}^S is the inter-cell interference at the user u caused by closest BS (no intra-cell interference on the downlink direction between different tiers is assumed) and expressed as follows:

$$\mathcal{I}_{su}^S = \begin{cases} \sum_{\substack{\tilde{m}=1 \\ \tilde{m} \neq m}}^M \left(\sum_{\substack{\tilde{u}=1 \\ \tilde{u} \neq u}}^U \epsilon_{\tilde{m}\tilde{u},n}^M P_{\tilde{m}\tilde{u},n}^M \right) h_{\tilde{m}u,n}^M, & \text{for ground tier,} \\ 0, & \text{for air tier,} \\ 0, & \text{for space tier,} \end{cases} \quad (10)$$

where $\epsilon_{m\tilde{u},n}^M$ is representing the exclusivity of the TBS m and RB allocation: $\epsilon_{m\tilde{u},n}^M = 1$, if RB n of nearby station is allocated to another user \tilde{u} from TBS m , and $\epsilon_{s\tilde{u},n}^S = 0$, otherwise. In fact, since the same RB might be allocated to the more than one user in different TBSs simultaneously in the ground tier, an inter-cell interference might be caused to some users. In (10), it can be noticed that the inter-cell interference is 0 for both air and space tier since we ignored this interference because the HAPs and satellite station are assumed to be equipped with different antennas and different beams that allow managing the resources in an efficient way by using different FSs for different ground cells [16].

Therefore, the BH data rate from station w to HAP l can be expressed as:

$$\bar{R}_{wl} = \delta_{wl} B_0 \log_2 \left(1 + \frac{P_0 g_{wl}}{\mathcal{N}_0 B_0} \right), \quad (11)$$

where B_0 and P_0 are the BH bandwidth and transmit power at station w , respectively.

III. PROBLEM FORMULATION

Our goal is to maximize the downlink data rate utility of ground users by optimizing the FH and BH associations, BSs' transmit power, and HAPs' locations. Based on the system parameters, the optimizer will determine whether using satellite station or HAPs would be more efficient than using TBSs. For remote areas or heavy loaded areas where the TBSs' would not able to support all ground users, the optimizer may decide to use the HAPs and satellite station when needed to support the ground users. This depends on many factors such as the users' location, number of the users to be served, and existence of the TBSs. For instance, if the users in remote areas outside the coverage of TBSs, then the satellite station and HAPs will try to accommodate these users. In the case of highly loaded networks, the optimizer is forced to use the network full capacity including the HAPs and satellite station in order to meet the users' demand. The optimization problem that we formulate will also optimize the locations of the HAPs and the BH association such that the throughput is maximized. Therefore, our optimization problem can be formulated as follows:

$$\begin{aligned} & \text{maximize} \quad \mathcal{U}(R_u) \\ & \quad \epsilon_{su,n}^S, \delta_{wl} \\ & \quad P_{su,n}^S, \mathbf{J}_l^L \end{aligned} \tag{12}$$

subject to:

$$0 \leq \sum_{n=1}^{N^S} \sum_{u=1}^U \epsilon_{su,n}^S P_{su,n}^S \leq \bar{P}_S, \quad \forall s, S \in \{M, L, 0\} \tag{13}$$

$$\sum_{n=1}^{N^L} \sum_{u=1}^U R_{lu,n}^L \leq \sum_{w=0}^W \bar{R}_{wl}, \quad \forall l, \tag{14}$$

$$\sum_{S \in \{M, L, 0\}} \sum_{s=1}^S \sum_{n=1}^{N^S} \epsilon_{su,n}^S \leq 1, \quad \forall u, \tag{15}$$

$$\sum_{u=1}^U \epsilon_{su,n}^S \leq 1, \quad \forall s, \forall S, \forall n = 1, \dots, N^S, \tag{16}$$

$$\sum_{w=0}^W \delta_{wl} = 1, \quad \forall l, \tag{17}$$

$$\sum_{l=0}^L \delta_{wl} \leq \bar{L}_w \quad \forall w, \tag{18}$$

where $\mathcal{U}(R_u)$ denotes the data rate utility of all users. Constraint (13) represents the peak power constraints at BS s . Constraint (14) represents the BH constraint of HAPs. Note that, we assume that the BH links of TBSs using fiber links and satellite station using feeder link are perfect, and hence not considering them in the BH constraint. Constraint (15) is to ensure that each ground user can be associated with one BS over one RB. Constraint (16) is to ensure there are no intra-cell interference between users associated to the same BS. Finally, constraints (17) and (18) represent the BH association conditions of HAPs.

A. Utility Selection

In this section, we characterize two different utility metrics that will be employed in the optimization problem given in (12)-(18).

1) **Max-Sum Utility (MSU)**: The utility of this metric is equivalent to the sum FH data rate of the ground users $\mathcal{U}(R_u) = \sum_{u=1}^U R_u$ as it promotes users with favorable channel gains and interference by allocating to them the best resources. On the other hand, using this utility will deprive users with bad channel gains and interference from the resources and thus they will have

very low data rates [26].

2) **Max-Min Utility (MMU)**: Due to the unfairness of MSU resource allocation, the need for more fair utility metrics arises. Max-min utility (MMU) is attempting to maximize the minimum data rate in the total network such as $\mathcal{U}(R_u) = \min_u(R_u)$ [27]. Note that, by increasing the priority of users having lower rates, MMU leads to more fairness in the network. In order to simplify the problem for this approach, we introduce a new decision variable $R_{\min} = \min_u(R_u)$. Therefore, our optimization problem can be re-formulated as:

$$\begin{aligned} & \underset{\substack{\epsilon_{su,n}^S, \delta_{wl} \\ P_{su,n}^S, \mathbf{J}_l^L, R_{\min}}}{\text{maximize}} && R_{\min} \end{aligned} \quad (19)$$

subject to:

$$R_u \geq R_{\min}, \quad \forall u, \quad (20)$$

(13), (14), (15), (16), (17), (18).

The formulated optimization problem in (12)-(18) is a mixed integer non-linear programming (MINLP), and solving it is a challenging task. In order to simplify the problem, we propose to solve it in two stages: short-term stage and long-term stage. In the former stage, we propose two solutions (near optimal and low complexity solutions) to find the best associations and transmit power allocations. While in the latter stage, the problem of optimizing the locations of HAPs is investigated.

IV. SHORT-TERM STAGE

In the short-term stage and considering fix HAPs' locations, we firstly solve for the FH associations (i.e., $\epsilon_{su,n}^S$) and BH associations (i.e., δ_{wl}) using uniform power distributions, i.e., $P_{su,n}^S = \bar{P}_S/N^S$. We then optimize the transmit powers of the BSs for these associations by approximating the optimization problem using Tyler expansion.

In the sequel, we propose two solutions in this stage. In the first solution, we propose a near optimal solution based on Taylor expansion approximation. While in the second solution, a low complexity heuristic approach using frequency partitioning (FP) technique is proposed, where we omit the inter-cell interference among TBSs and, thus, solve the problem quickly.

A. Near Optimal Solution

In fact, by fixing the transmit powers, it can be seen that the optimization problem becomes linear binary optimization problem in terms of $\epsilon_{su,n}^S$ and δ_{wl} , except (12) which is non linear with respect to $\epsilon_{su,n}^S$ due to the existence of the \mathcal{I}_{mu}^M term in (10). On the other hand, by fixing $\epsilon_{su,n}^S$ and δ_{wl} , the optimization problem is convex problem in $P_{su,n}^S$ except constraints (12) and (14). Therefore, in order to solve the problem iteratively (solving the associations and them transmit powers), the goal is to linearize (12) respects to $\epsilon_{su,n}^S$ with fixed $P_{su,n}^S$. Then, approximate (12) and (14) to convex ones respects to $P_{su,n}^S$ with fixed $\epsilon_{su,n}^S$ and δ_{wl} .

It can be notice that \mathcal{I}_{mu}^M in (10) can be re-write as $\sum_{\substack{\tilde{m}=1 \\ \tilde{m} \neq m}}^M \left(\sum_{\substack{\tilde{u}=1 \\ \tilde{u} \neq u}}^U P_{\tilde{m}\tilde{u},n}^M \right) h_{\tilde{m}u,n}^M$ by adding the following constraint:

$$0 \leq P_{\tilde{m}\tilde{u},n}^M \leq \epsilon_{\tilde{m}\tilde{u},n}^M \bar{P}_M, \quad \forall \tilde{m}, \forall \tilde{u}. \quad (21)$$

Now, the optimization problem becomes a linear one with respect to $\epsilon_{su,n}^S$ and δ_{wl} and thus, it can be solved using on-the-shelf softwares such as Gurobi/CVX interface [28].

On the other hand, by fixing the association variables (i.e., $\epsilon_{su,n}^S$ and δ_{wl}), the optimization problem in (12)-(18) can be re-write as:

$$\underset{P_{su,n}^S}{\text{maximize}} \quad \mathcal{U}(R_u) \quad (22)$$

subject to:

$$0 \leq \sum_{n=1}^{N^S} \sum_{u=1}^U \epsilon_{su,n}^S P_{su,n}^S \leq \bar{P}_S, \quad \forall s, S \in \{M, L, 0\} \quad (23)$$

$$\sum_{n=1}^{N^L} \sum_{u=1}^U R_{lu,n}^L \leq \sum_{w=0}^W \bar{R}_{wl}, \quad \forall l. \quad (24)$$

It can be noticed that the optimization problem (22)- (24) is convex problem in $P_{su,n}^S$ except constraints (22) and (24). Therefore, the goal is to convert these constraints into convex ones in terms of $P_{su,n}^S$ in order to solve the power optimization problem efficiently.

1) *Approximation of The Objective Function (22)*: : Let us start with objective function (22) by expanding it as follows:

$$\begin{aligned}
R_u = & B^M \sum_{m=1}^M \sum_{n=1}^{N^M} \epsilon_{mu,n}^M \log_2 \left(1 + \frac{P_{mu,n}^M h_{mu,n}^M}{\mathcal{I}_u^M + \mathcal{N}_0 B^M} \right) + \\
& B^L \sum_{l=1}^L \sum_{n=1}^{N^L} \epsilon_{lu,n}^L \log_2 \left(1 + \frac{P_{lu,n}^L h_{lu,n}^L}{\mathcal{N}_0 B^L} \right) + \\
& B^0 \sum_{n=1}^{N^0} \epsilon_{0u,n}^0 \log_2 \left(1 + \frac{P_{0u,n}^0 h_{0u,n}^0}{\mathcal{N}_0 B^0} \right). \tag{25}
\end{aligned}$$

In (25), since we are maximizing the utility, then we need the function to be concave. Note that the second and third terms are concave functions in terms of $P_{lu,n}^L$ and $P_{0u,n}^0$. In order to convert the objective function to a concave function, the first term in (25) needs to be concave it terms of $P_{mu,n}^M$. Let us start by expanding the first term in (25) as follows:

$$\begin{aligned}
R_{mu,n}^M = & \underbrace{\epsilon_{mu,n}^M B^S \log_2 \left(\mathcal{N}_0 B^S + \sum_{m=1}^M \sum_{u=1}^U P_{mu,n}^M h_{mu,n}^M \right)}_{\hat{R}_{mu,n}^M} \\
& - \underbrace{\epsilon_{mu,n}^M B^S \log_2 \left(\mathcal{N}_0 B^S + \sum_{\substack{\tilde{m}=1 \\ \tilde{m} \neq l}}^M \sum_{\substack{\tilde{u}=1 \\ \tilde{u} \neq u}}^U \epsilon_{\tilde{m}\tilde{u},n}^M P_{\tilde{m}\tilde{u},n}^M h_{\tilde{m}\tilde{u},n}^M \right)}_{\check{R}_{mu,n}^M}. \tag{26}
\end{aligned}$$

Note that $\hat{R}_{mu,n}^M$ is concave, because the log of an affine function is concave [29]. Also, $\check{R}_{mu,n}^M$ is a convex function, and thus, it needs to be converted to a concave function. To tackle the non-concavity of $\check{R}_{mu,n}^M$, the successive convex approximation (SCA) technique can be applied where in each iteration, the original function is approximated by a more tractable function at a given local point as given in algorithm 1. Recall that $\check{R}_{mu,n}^M$ is convex in $P_{\tilde{m}\tilde{u},n}^M$, and any convex function can be globally lower-bounded by its first order Taylor expansion at any point. Therefore, given $P_{\tilde{m}\tilde{u},n}^M(r)$ in iteration r , we obtain the following lower bound for $\check{R}_{mu,n}^M(r)$:

$$\begin{aligned}
\check{R}_{mu,n}^M(r) \geq & -\epsilon_{mu,n}^M B^S \log_2(\psi(r)) \\
& - \frac{\epsilon_{\tilde{m}\tilde{u},n}^M h_{\tilde{m}\tilde{u},n}^M}{\ln(2)\psi(r)} (P_{\tilde{m}\tilde{u},n}^M - P_{\tilde{m}\tilde{u},n}^M(r)), \tag{27}
\end{aligned}$$

where $\psi(r) = \mathcal{N}_0 B^S + \sum_{\substack{\tilde{m}=1 \\ \tilde{m} \neq l}}^M \sum_{\substack{\tilde{u}=1 \\ \tilde{u} \neq u}}^U \epsilon_{\tilde{m}\tilde{u},n}^M P_{\tilde{m}\tilde{u},n}^M h_{\tilde{m}\tilde{u},n}^M$. Now it can be seen that the objective function in (25) is a concave function in terms of $P_{su,n}^S$.

Algorithm 1 SCA Algorithm

Select feasible initial values $P_{\tilde{m}u,n}^M$.

$r=1$.

repeat

Solve the optimization problem (22)-(24) using the interior-point method to determine the new approximated solution $P_{\tilde{m}u,n}^M(r)$.

until Convergence.

2) *Approximation of Constraint (24)*: : We can approximate this constraint by ensuring that the data rate from HAP l to any associated users u is smaller than the average BH constraint. In other words, constraint (14) can be approximated as:

$$\sum_{n=1}^{N^L} \epsilon_{lu,n}^L \left(1 + \frac{P_{lu,n}^L h_{lu,n}^L}{\mathcal{N}_0 B^S} \right) \leq \frac{\omega}{\sum_{n=1}^{N^L} \epsilon_{lu,n}^L}, \quad \forall l, \forall u, \quad (28)$$

where $\omega = 2^{(\sum_{w=0}^W \bar{R}_{wl})/B^S}$.

Now, our power allocation optimization problem given in (22)-(24) becomes convex problem in respect to $P_{su,n}^S$ for fix associations and HAPs' locations. Thus, the duality gap of our convex power allocation problem in OFDMA system is zero. Hence, We can solve our convex transmit power allocation optimization problem by exploiting its strong duality.

B. Low Complexity Solution

In subsection, we propose a low complexity and efficient technique to mitigate the inter-cell interference between users associate to different TBSs in the ground tier. We divide the users into two groups, 1) center users: users located in areas close to the center of the TBSs' cells and 2) edge users: users located in the edges of the TBSs' cells. We assume that TBSs can be associated with the center users only. In this case, inter-cell interference is assumed to be $\mathcal{I}_{mu}^M = 0$ due to large distances between users that using the same frequency bands in the ground tier. Hence, the association problem is linear and we can omit constraint (21). On the other hand, the edge users can be served by the HAPs and satellite station as shown in Fig 3. Hence, (22) becomes a convex function with respect to $P_{su,n}^S$.

Therefore, the formulated optimization problem in (12)- (14) is a linear assignment problem with respect to $\epsilon_{su,n}^S$ and δ_{wl} and can be solved efficiently by using the Hungarian algorithm with complexity of $(MN^M + LN^L + N^0)^3$ [30].

On the other hand, by only approximating (24), the formulated optimization problem in (22)-(24) becomes a convex optimization problem in terms of $P_{su,n}^S$. Therefore, it can be solved efficiently by solving the its dual problem.

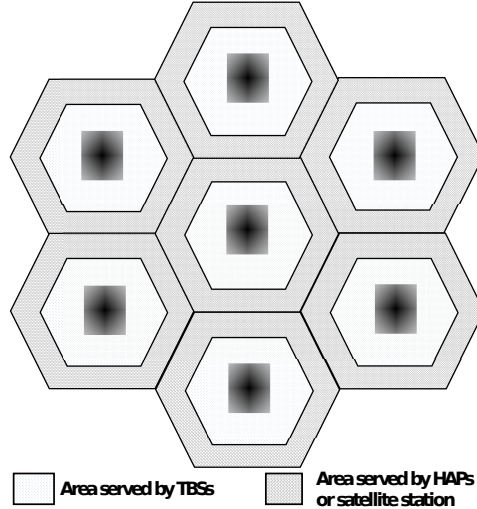


Fig. 3: Frequency partitioning technique.

V. LONG-TERM STAGE

Due to the non-convexity of the formulated optimization problem (12)-(18) even with fixed associations and BSs transmit powers, we introduce a low complexity and efficient algorithm based on the SR process. The proposed algorithm has many advantages over other heuristic algorithms proposed in the literature such as simple implementation, low complexity, and quick convergence to a near optimal solution. Furthermore, since we solve this problem for long-term stage, where the time slots are relatively long compared to the channel coherence time and hence, we focus on the average statistics (such as average channel gains) of the network. This implies that average users' throughput is assumed instead of instantaneous throughput.

We start our algorithm by generating initial next position candidates $T_l, \forall l$ as a circle with radius $r(i)$ around all current locations of the HAPs to form the initial population. Next, we solve the average associations and transmit powers of the BSs to determine maximum number of average users inside the HAPs coverage areas for each candidates combination. In other

words, determine the value $U_{\max}^L = \sum_{l=1}^L \sum_{n=1}^{N^S} \sum_{u=1}^U \epsilon_{lu,n}^L$, after excluding the users associated to TBSs. We then find the initial best local candidate combinations $T^{i,\text{local}} = t_l^{i,\text{local}}, \forall l$ that gives the maximum number of users associated with HAPs for iteration i . After that, we apply the SR process recursively to find the best global solution $T^* = t_l^*, \forall l$ by generating a new candidates on a circle of radius $(r(i+1)=r(i)/2)$ around each local solution. We repeat this process until the size of the sample space decreases below a certain threshold I_{\max} or no improvement can be made. Fig. 4 shows an example of the proposed algorithm using two HAPs ($L = 2$), $T = 4$, and three maximum iteration $I_{\max} = 3$. The details of the HAPs' locations algorithm that optimize the locations of the HAPs based on average users' locations are given in Algorithm 2.

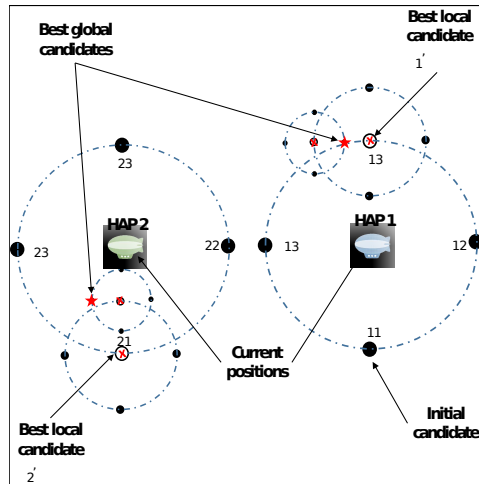


Fig. 4: Proposed heuristic approach.

VI. SIMULATION RESULTS

In this section, selected simulation results are provided to demonstrate the advantages of our proposed solution. The simulation results are set within area of $180 \text{ Km} \times 180 \text{ Km}$. Within this area, U users are distributed in three different subareas (i.e., subarea 1: 30 Km^2 , subarea 2: 30 Km^2 , and subarea 3: the remaining) with different dense distributions. Subarea 1 contains $M = 9$ TBSs with coordinates are: x: (75 Km to 105 Km), and y: (0 Km to 30 Km) and contains 40% of the total number of users. Subarea 2, has no TBSs with coordinates are: x: (75 Km to 105 Km), and y: (150 Km to 180 Km) and contains 30% of the total number of users. In other words, subarea 2 has dense users but with no infrastructure (e.g., it ca flying at a fixed altitude be an area with a damaged infrastructure or temporarily high traffic area). While subarea

Algorithm 2 HAPs' Locations Algorithm

```

1:  $i=1$ .
2: Generate initial candidates  $T$  in a circle of radius  $r = r(i)$  around each HAP  $J_l^L(t_l)$ ,  $l = 1 \cdots L$ .
3: while Not converged or reaching  $I_{\max}$  do
4:   for  $l = 1 \cdots L$  do
5:     for  $t_l = 1 \cdots T$  do
6:       Find the optimized value of  $\epsilon_{su,n}^S$ ,  $\delta_{wl}$ , and  $P_{su,n}^S$  as explained in Section. IV for average statistics.
7:       Compute  $U_{\max}^L = \sum_{l=1}^L \sum_{n=1}^{N^S} \sum_{u=1}^U \epsilon_{lu,n}^L$ .
8:     end for
9:   end for
10:  Find  $t_l^{i,\text{local}} = \arg \max_{t_l} U_{\max}^L$ , (i.e.,  $t_l^{i,\text{local}}$  indicates the index of the best local candidate that results in the highest  $U_{\max}^L$  for iteration  $i$ ).
11:   $r = r(i)/2$ 
12:  Start applying SR process for the local solution.
13:   $i=i+1$ .
14: end while

```

3 is the remaining area and contains 30% of the total number of users. For example, subarea 1 and subarea 2 can be considered as urban areas with and without TBSs, respectively, while subarea 3 can be considered as rural are. The satellite station is assumed to be in a fixed location with the coordinate [90,90,2000] Km. Also, we consider $L = 5$ HAPs flying at a fixed altitude $z_l^L = 18$ Km, $\forall l = 1, \dots, L$. We assume that the HAPs initially start at location $\mathbf{J}_1^L = [90, 90, 18]$ Km, $\mathbf{J}_2^L = [30, 30, 18]$ Km, $\mathbf{J}_3^L = [150, 30, 18]$ Km, $\mathbf{J}_4^L = [30, 150, 18]$ Km, $\mathbf{J}_5^L = [150, 150, 18]$ Km. We assume that $W = 4$ and located in the four corners of the desired area. We assume $N^M = 50$, $N^L = 100$, and $N^0 = 200$ available RBs in the FH in our simulations. The maximum transmit power of TBS, HAP, and satellite station are, respectively, given as $\{40,100,250\}$ W. The noise power N_0 is assumed to be -174 dBm. In Table II, we present the values of the remaining environmental parameters used in the simulations unless otherwise stated [14], [15], [23].

Fig. 5 plots the optimization of HAPs' locations and BH associations using average users location for two high and low users densities with $P_0 = 40$ W, $B_0 = 4$ MHz, and $\bar{P}_l = 100$ W. The figure also shows the BH association of HAPs with the GWs. For instance, Fig. 5-a shows that the HAPs try to accommodate maximum number of users by finding the best HAPs'

locations that improved the FH and BH links at the same time. Note that the users located outside the coverage areas of HAPs and TBSs are associated with satellite station. While, in the case of low dense users, HAPs try to associated with all users as shown in Fig. 5-b. This is can explained by the fact that associating with HAPs, in general, provide a better data rate instead of associating to satellite station due to the high path-loss attenuation between satellite station and ground users. In this case, the HAPs can provide services to ground users with much lower delay and higher throughput.

Fig. 6 plots the average data rate per user (i.e., $\sum_{u=1}^U I(U)$) versus total number of users (i.e., subarea 1: 40%, subarea 2: 30%, subarea 3: 30%) with $P_0 = 40$ W, $B_0 = 4$ MHz, and $\bar{P}_l = 100$ W. Our proposed solutions (i.e., approximated and low complexity solutions) are compared with two benchmark solutions: 1- optimizing only the FH and BH associations and the HAPs' locations with uniform power distribution (i.e., $P_{su,n}^S = \bar{P}_S/N^S$), and 2- optimizing only the placement of the HAPs using random FH and BH associations with uniform power distribution. The figure shows that for fixed resources, as U increases, the average data rate decreases due to the limitation of the available resources. Furthermore, the figure shows that the approximate solution and low complexity solution achieve almost the same performance for low values of U . However, there will be a gap between the two proposed solutions when U is relatively large. This is can be explained by the fact that the low complexity solution forces some HAPs to cover the TBSs coverage areas in order to implement the frequency partitioning technique as shown in Fig. 3. This will not effect the performance when U is relatively low, but when U is large, and because of the limitation number of HAPs, then the HAPs located in the TBSs coverage areas maybe be better to move to different locations. Thanks to the HAPs, because HAPs have large coverage areas of HAP, this gap for large U is still acceptable. This figure also shows that our proposed solutions outperform the other two benchmarks solutions. For instance, using

TABLE II: Simulation parameters

Constant	Value	Constant	Value	Constant	Value
f_c^M (GHz)	1.8	f_c^L (GHz)	3.0	f_c^0 (GHz)	5.0
f_c (GHz)	3.4	χ	2	κ_L, κ_0	10
B^M (kHz)	1.8	B^L (MHz)	1.0	B^L (MHz)	2.0
Ω_0	0.372	Ω_1	0.0129	Ω_2	7.64

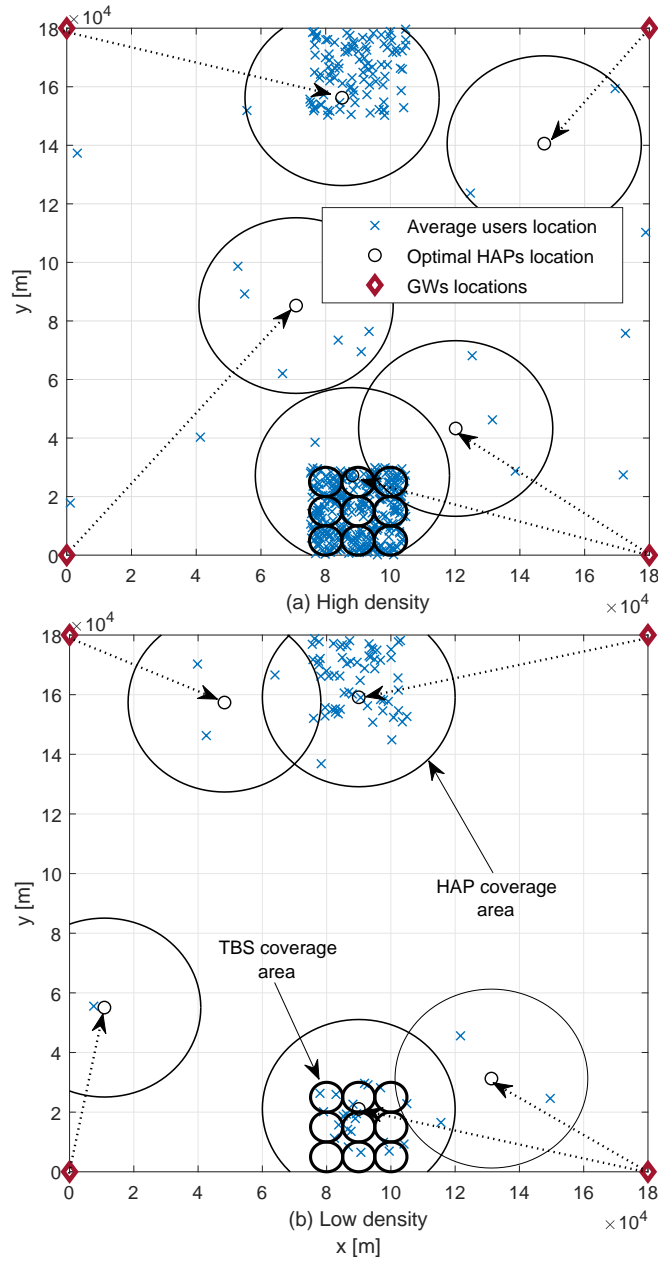


Fig. 5: HAP placement optimization with BH associations.

$U = 400$, our proposed solution can enhance the average rate throughput by at least 39% and 88% compared to optimize the associations with uniform power and to random associations with uniform power, respectively. Furthermore, it can be noticed that the gap between the proposed solutions and benchmarks solutions is increased as U increases. This is due to the fact, as U increases, the need of managing and optimizing the power is needed more.

All simulations show that MSU leads to the highest average data rate in the system. However,

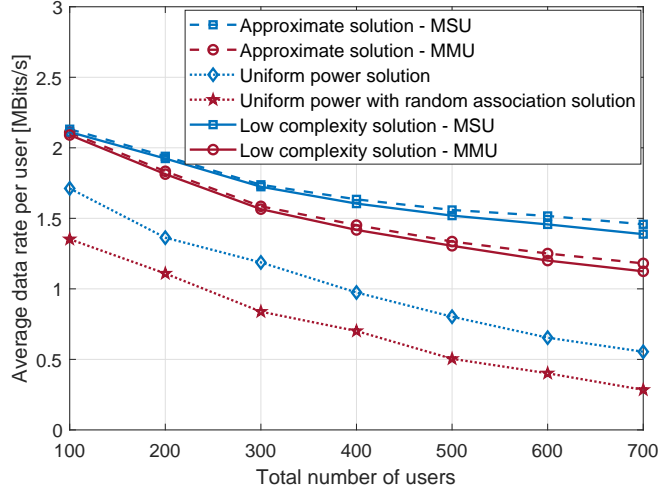


Fig. 6: Average data rate per user as a function of number of users.

this comes at the expense of fairness as it is shown in Table III. Indeed, the table compares between the two different utilities for the same channel realization with fixed $P_0 = 40$ W, $B_0 = 4$ MHz, $\bar{P}_l = 100$ W, and $U = 400$ (for this realization, 160 user associated to TBSs, 172 user associated to HAPs 172, and 68 user associated to satellite station). In Table III, we denote \bar{R}^S , R_{\max}^S , and R_{\min}^S as average rate, maximum rate, and minimum rate in tier S , respectively. Also, P_{\max}^S and P_{\min}^S denoted as maximum and minimum transmit powers in tier S . By using one realization, it can be shown that MSU enhances the average data rate, by allocating most of the resources to users having the best channel conditions. On the other hand, MMU approach maximizes the minimum data rate and provides almost the same rate for all users. Hence, MMU leads to more fairness performance. The choice of the utility is related to the service given to the users. For instance, if the application requires same downlink rates between users, then MMU can be used. on the other hand, if it consists in a pure transmission without priorities, then MSU could be employed.

Fig. 7 and Fig. 8 illustrate the performance of the average data rate for users associated with HAPs using $U = 400$. For instance, Fig. 7 plots the effect of the BH bandwidth B_0 on the average data rate of HAPs' users for different BH transmit powers $P_0 = \{10, 20, 30, 40\}$ W with $\bar{P}_l = 100$ W. This figure shows that the average data rate of HAPs' users is improving with the increase of B_0 up to a certain cutoff value, that depends on the BH rate constraint as given in 14. This is due to the fact that starting from this point of B_0 the average data rate

TABLE III: Comparison between MSU and MMU for fixed $P_0 = 40$ W, $B_0 = 4$ MHz, $\bar{P}_l = 100$ W, and $U = 400$

	Users associated with	\bar{R}^S Mbits/s	(R_{\max}^S, P_{\max}^S) (Mbits/s, W)	(R_{\min}^S, P_{\min}^S) (Mbits/s, W)
MSU	TBSs	2.14	(4.13, 15.25)	($\sim 0, \sim 0$)
	HAPs	1.92	(3.19, 39.70)	(.0415, 1.2)
	Satellite	(0.016)	(0.085, 97.53)	($\sim 0, \sim 0$)
MMU	TBSs	(1.91)	(1.96, 5.49)	(1.88, 8.20)
	HAPs	(1.50)	(1.81, 3.91)	(1.39, 4.5)
	Satellite	(0.01)	(0.01, 4.81)	(0.01, 4.65)

can not be enhanced further because it depends on the value of $P_{lu,n}^L$ which is limited by \bar{P}_L as given in (13). Also, Fig. 7 shows that the cutoff value depends on the BH transmit power P_0 . As P_0 increases the corresponding B_0 value of the cutoff value decreases in order to respect constraint 14. In this case, the bottleneck is the FH rate constraint which is limited by \bar{P}_L .

On the other hand, to illustrate the BH bottleneck, Fig. 8 plots the average data rate of HAPs' users versus HAPs' peak power \bar{P}_L using $P_0 = 40$ W. The figure shows that as \bar{P}_l increases, the average data rate is increases up to a certain point. This can be explained by starting from this point of \bar{P}_l , the average data rate can not be improved because it depends also on the BH data rate constraint \bar{R}_{wl} as given in 14. Furthermore, it can be noticed that the average data rate is enhanced as B_0 increases due to the reason, that increasing B_0 will also increase the value of \bar{R}_{wl} and thus, increase the BH bottleneck.

Finally, Fig. 9 plots the convergence speed of the SR algorithm, defined by the number of iterations needed to reach convergence, for both utilities, MSU and MMU. Note that one iteration in Fig. 9 corresponds to one iteration of the while loop given in Algorithm 2 line 4-13. It can be noticed that the algorithm is converge within around 8-13 iterations.

VII. CONCLUSION

This paper proposed an efficient optimization framework using TBSs, HAPs, and satellite station to provide connectivity to the ground users taking into consideration the BH limitation. The objective was to maximize the users' throughput by optimizing the front-hauling and back-hauling associations, transmit powers of the base stations, and the HAPs' locations. We proposed an approximate and a low complexity solutions to optimally determine the decision variables.

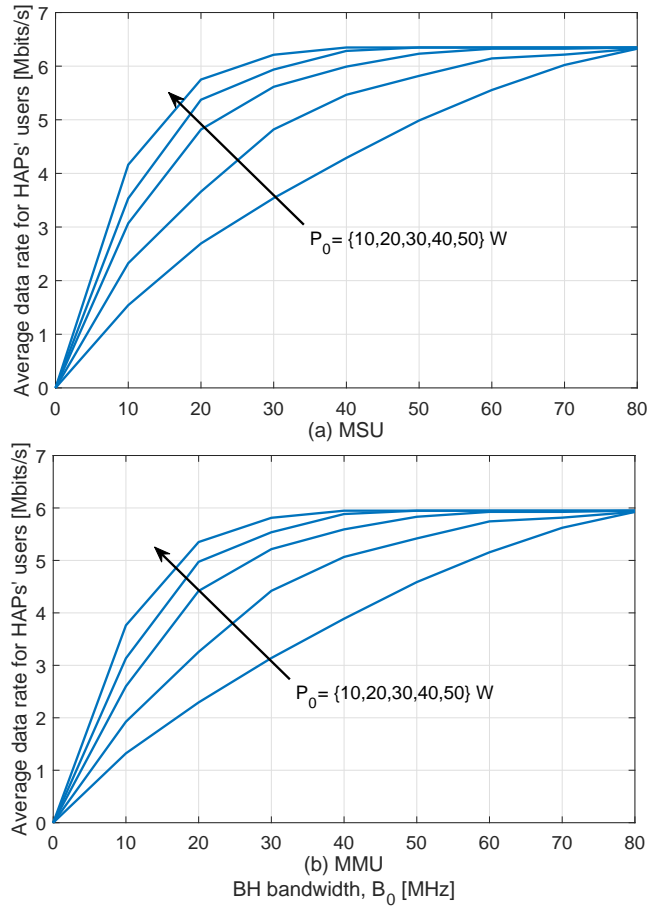


Fig. 7: Average data rate of HAPs' users versus BH bandwidth.

The simulation results illustrated the behavior of our approach and their significant impacts on the users' throughput. In our next challenging task, a free-space optical (FSO) communication link between GW and HAPs will be considered in order to mitigate the BH bottleneck limitation thus enhance the performance. However, it will add more complexity to the problem by optimizing extra parameters such as the LoS angles.

REFERENCES

- [1] X. Yan, H. Xiao, C. Wang, and K. An, "Outage performance of NOMA-based hybrid satellite-terrestrial relay networks," *IEEE Wireless Communications Letters*, vol. 7, no. 4, pp. 538–541, Aug. 2018.
- [2] K. An, M. Lin, T. Liang, J. Wang, J. Wang, Y. Huang, and A. L. Swindlehurst, "Performance analysis of multi-antenna hybrid satellite-terrestrial relay networks in the presence of interference," *IEEE Transactions on Communications*, vol. 63, no. 11, pp. 4390–4404, Nov. 2015.

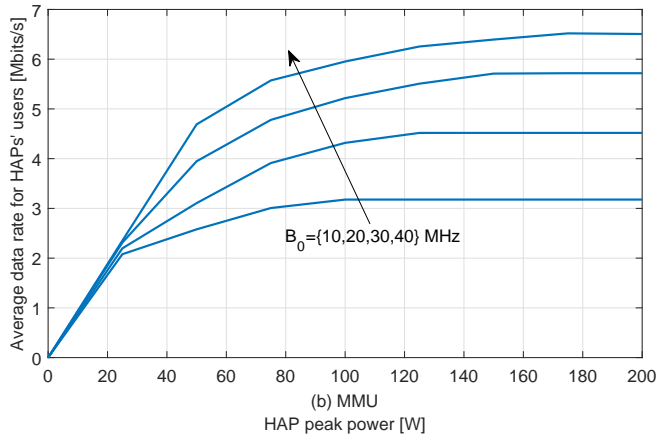
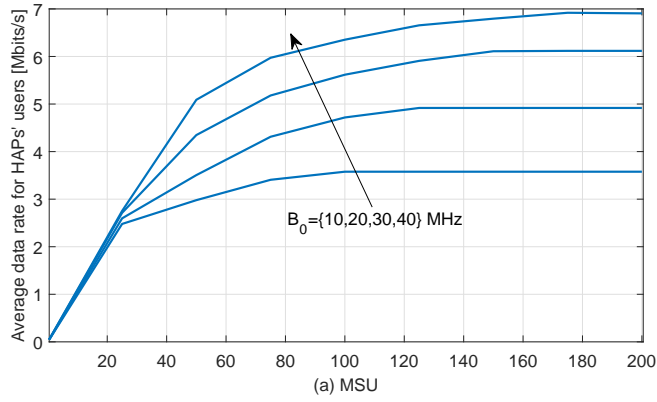


Fig. 8: Average data rate of HAPs' users versus HAPs' peak power.

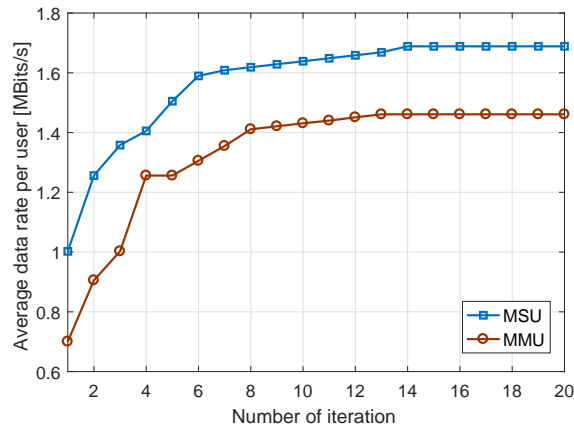


Fig. 9: Convergence of the proposed SR algorithm.

- [3] U. Park, H. W. Kim, D. S. Oh, and B. J. Ku, "Flexible bandwidth allocation scheme based on traffic demands and channel conditions for multi-beam satellite systems," in *Proc. of the IEEE Vehicular Technology Conference (VTC Fall)*, Quebec City, QC, Canada, Sep. 2012, pp. 1–5.

- [4] J. Lei and M. A. Vazquez-Castro, "Joint power and carrier allocation for the multibeam satellite downlink with individual SINR constraints," in *Proc. of the IEEE International Conference on Communications (ICC), Cape Town, South Africa*, May 2010, pp. 1–5.
- [5] F. Li, K. Lam, J. Hua, K. Zhao, N. Zhao, and L. Wang, "Improving spectrum management for satellite communication systems with hunger marketing," *IEEE Wireless Communications Letters*, vol. 8, no. 3, pp. 797–800, June 2019.
- [6] X. Cao, P. Yang, M. Alzenad, X. Xi, D. Wu, and H. Yanikomeroglu, "Airborne communication networks: A survey," *IEEE Journal on Selected Areas in Communications*, vol. 36, no. 9, pp. 1907–1926, Sep. 2018.
- [7] A. Mohammed, A. Mehmood, F. Pavlidou, and M. Mohorcic, "The role of high-altitude platforms (HAPs) in the global wireless connectivity," *Proceedings of the IEEE*, vol. 99, no. 11, pp. 1939–1953, Nov 2011.
- [8] H. Lu, Y. Gui, X. Jiang, F. Wu, and C. W. Chen, "Compressed robust transmission for remote sensing services in space information networks," *IEEE Wireless Communications*, vol. 26, no. 2, pp. 46–54, Apr. 2019.
- [9] —, "Compressed robust transmission for remote sensing services in space information networks," *IEEE Wireless Communications*, vol. 26, no. 2, pp. 46–54, Apr. 2019.
- [10] S. Karapantazis and F. Pavlidou, "Broadband communications via high-altitude platforms: A survey," *IEEE Communications Surveys Tutorials*, vol. 7, no. 1, pp. 2–31, First Quarter 2005.
- [11] J. Marriott, B. Tezel, Z. Liu, and N. Stier, "Trajectory optimization of solar-powered high-altitude long endurance aircraft," *Facebook Research*, Oct. 2018.
- [12] J. Marriott and B. Thomsen, "Energy-optimized trajectory planning for high altitude long endurance (HALE) aircraft," *Facebook Research*, Oct. 2018.
- [13] Z. Yang and A. Mohammed, "Wireless communications from high altitude platforms: Applications, deployment, and development," in *Proc. of the 12th IEEE International Conference on Communication Technology, Nanjing, China*, Nov. 2010, pp. 1476–1479.
- [14] R. Zong, X. Gao, X. Wang, and L. Zongting, "Deployment of high altitude platforms network: A game theoretic approach," in *Proc. of the International Conference on Computing, Networking and Communications (ICNC), Maui, HI, USA*, Jan. 2012, pp. 304–308.
- [15] A. Ibrahim and A. S. Alfa, "Using Lagrangian relaxation for radio resource allocation in high altitude platforms," *IEEE Transactions on Wireless Communications*, vol. 14, no. 10, pp. 5823–5835, Oct. 2015.
- [16] D. Grace, J. Thornton, Guanhua Chen, G. P. White, and T. C. Tozer, "Improving the system capacity of broadband services using multiple high-altitude platforms," *IEEE Transactions on Wireless Communications*, vol. 4, no. 2, pp. 700–709, Mar. 2005.
- [17] J. Tong, Y. Lu, D. Zhang, G. Cui, and W. Wang, "Max-min analog beamforming for high altitude platforms communication systems," in *Proc. of the IEEE International Conference on Communications in China (ICCC), Beijing, China*, Aug. 2018, pp. 872–876.
- [18] Z. Chen, T. B. Lim, and M. Motani, "HAP-assisted LEO satellite downlink transmission: An energy harvesting perspective," in *Proc. of the 15th IEEE International Workshop on Signal Processing Advances in Wireless Communications (SPAWC), Toronto, ON, Canada*, June 2014, pp. 194–198.
- [19] S. Zhou, G. Wang, S. Zhang, Z. Niu, and X. S. Shen, "Bidirectional mission offloading for agile space-air-ground integrated networks," *IEEE Wireless Communications*, vol. 26, no. 2, pp. 38–45, Apr. 2019.
- [20] 3rd Generation Partnership Project, "Evolved universal terrestrial radio access E-UTRA; Physical channels and modulation," 3GPP TS 36.211 3GPP V 11.2.0, Release 11, Apr. 2013.
- [21] D. A. J. Pearce and D. Grace, "Optimum antenna configurations for millimetre-wave communications from high-altitude platforms," *IET Communications*, vol. 1, no. 3, pp. 359–364, June 2007.

- [22] E. Falletti, M. Laddomada, M. Mondin, and F. Sellone, "Integrated services from high-altitude platforms: A flexible communication system," *IEEE Communications Magazine*, vol. 44, no. 2, pp. 85–94, Feb. 2006.
- [23] A. Abdi, W. C. Lau, M.-S. Alouini, and M. Kaveh, "A new simple model for land mobile satellite channels: First- and second-order statistics," *IEEE Transactions on Wireless Communications*, vol. 2, no. 3, pp. 519–528, May 2003.
- [24] A. Iqbal and K. M. Ahmed, "Outage probability analysis of multi-hop cooperative satellite-terrestrial network," in *Proc. of the 8th Electrical Engineering/ Electronics, Computer, Telecommunications and Information Technology (ECTIT) Association, Phuket, Thailand*, May 2011, pp. 256–259.
- [25] F. Dong, H. Li, X. Gong, Q. Liu, and J. Wang, "Energy-efficient transmissions for remote wireless sensor networks: An integrated HAP/satellite architecture for emergency scenarios," *Sensors*, vol. 15, no. 9, pp. 22 266–22 290, 2015.
- [26] X. Bi, J. Zhang, Y. Wang, and P. Viswanath, "Fairness improvement of maximum C/I scheduler by dumb antennas in slow fading channel," in *Proc. of the 72nd IEEE Vehicular Technology Conference (VTC Fall), Ottawa, Ontario, Canada*, Sep. 2010, pp. 1–4.
- [27] Y. Song and G. Li, "Cross-layer optimization for OFDM wireless networks-Part I: Theoretical framework," *IEEE Transactions on Wireless Communications*, vol. 4, no. 2, pp. 614–624, Apr. 2005.
- [28] "Gurobi Optimizer Reference Manual," 2016. Available [online]: <http://www.gurobi.com/>.
- [29] S. Boyd and L. Vandenberghe, *Convex Optimization*. New York, NY, USA: Cambridge University Press, 2004.
- [30] H. W. Kuhn, "The Hungarian Method for the Assignment Problem," *50 Years of Integer Programming 1958-2008*. Berlin, Heidelberg, ch2. 2010.